Available online at www.sciencedirect.com

SciVerse ScienceDirect

Ceramics International 38 (2012) 5181–5188

CERAMICS INTERNATIONAL

www.elsevier.com/locate/ceramint

# Studies on the properties of $Ni_{0.6}Cu_{0.4}Mn_2O_4$ NTC ceramic due to Fe doping

R.N. Jadhav, S.N. Mathad, Vijaya Puri *

*Thick and Thin Film Device Lab, Department of Physics, Shivaji University, Kolhapur 416004, India*

Received 26 November 2011; received in revised form 6 March 2012; accepted 7 March 2012
Available online 16 March 2012

**Abstract**

The influence of the Fe on the microstructure, electrical and dielectric properties of $Ni_{0.6}Cu_{0.4}Fe_yMn_{2-y}O_4$ ($0.1 \leq y \leq 0.5$) negative temperature coefficient (NTC) thermistors prepared by well known simple chemical co-precipitation method were studied. The replacement of manganese by iron plays an important role in changing the lattice parameter, X-ray density, sintered density, porosity, DC resistivity at different temperatures and dielectric properties at different frequencies. The X-ray and sintered density increased linearly and porosity decreased with iron. The room temperature resistivity of nickel copper manganite NTC ceramic decreased from 1 MΩ cm to 68 KΩ cm and dielectric constant increased from $\sim 9 \times 10^7$ to $1.5 \times 10^9$ at 20 Hz as iron content increased.


*Keywords:* C. Electrical properties; C. Dielectric properties; NTC thermistor; Nickel-copper manganite

## 1. Introduction

Monitoring and control of temperature is of paramount importance in of our daily life. Temperature sensors are ubiquitous not only in domestic and industrial activities but also in laboratory and medical procedures. An assortment of temperature sensors is commercially available for such purposes. NTC thermistors find extensive use in circuit compensation, aerospace, cryogenic, automotive temperature measurement and control applications [1,2]. The spinel materials have been widely used in industry as a temperature sensor in bulk material applications [3,4]. In sensor technologies, ceramics are very useful crystalline materials because of their structural strength, thermal stability, light weight, resistance to many chemicals, ability to bond with other materials, and excellent electrical properties. Manganese based spinel semi-conducting ceramics have been studied as a NTC thermistors due to its interesting electrical properties. Low cost, ease of manufacturing and interesting thermistor properties make polycrystalline nickel manganite one of the most important ceramics today, which exhibit a uniform exponential decrease of resistance with increasing temperature up to ~300 °C, i.e. a negative temperature coefficient of resistance (NTCR) [5,6] which makes the oxide well suited for use as a NTC thermistor material in specific temperature sensors and attenuators.

Nickel manganite ($NiMn_2O_4$) crystallizes in the cubic spinel structure, having structural formula $AB_2O_4$ based upon the cubic close packing of oxygen ions in which cations are situated on both tetrahedral (A-sites) and octahedral (B-sites) sites [7]. In nickel manganite the electrical conductivity is satisfactorily described by a phonon assisted hopping of charge carriers between $Mn^{3+}$ and $Mn^{4+}$ ions on octahedral sites of spinel structure induced by lattice vibrations. The symmetry of the spinel structure as well as the site occupation is strongly dependent on the 3d transition metals used for the synthesis of the ceramic and also on the manufacturing conditions and there are some reports available describing the structural and electrical properties of nickel manganite [8,9].

Extensive studies have been reported on the modification of nickel manganite NTC thermistor. Modification of thermistor characteristics is generally done by doping suitable ions or by changing the processing conditions like sintering temperature, rate of cooling, duration of sintering, etc. [10–12]. Modifying and controlling these factors allow tuning the resistivity of the materials and also their thermistor constant ($\beta$ value) [13]. In terms of fundamental research, most work has been devoted to the basic structural, electrical, and magnetic characterization of

* Corresponding author. Fax: +91 231 2691533.
*E-mail address:* vijayapuri1@gmail.com (V. Puri).

0272-8842/$36.00 
doi:10.1016/j.ceramint.2012.03.024

NTCR thermistors based on doped $NiMn_2O_4$ ceramics. Iron plays an important role in the physical and electrical properties of nickel manganite. Effect of Fe doping and of binder variation on electrical and microwave properties have been reported [14]. It is also reported that owing to the fact that Fe ion has some specialties, such as changeable valency $Fe^{2+}$ and $Fe^{3+}$, the flexible occupation of sublattices in spinel structure A- and B-sites, Fe ion has complicated influence on the magnetic and electrical properties of the electroceramics [15–17]. Park et al. [18] reported that introduction of $Fe^{3+}$ ion into ternary system may produce interesting change during the electrical properties in NTC thermistors. It is observed that iron plays the important role in NTC thermistor but very few reports are available to study the effect of Fe substituted on electrical and dielectric properties of NTC thermistor.

The present study focuses on the synthesis of $Ni_{0.6}Cu_{0.4}Fe_yMn_{2-y}O_4$ where $y = 0.1, 0.2, 0.3, 0.4, 0.5$ NTC thermistor compositions and to correlate the effect of iron concentration on the lattice parameter, X-ray density, sintered density, porosity, grain size, DC electrical resistivity, thermistor constant, activation energy and dielectric constant.

## 2. Experimental

Ultrafine powders of iron doped nickel copper manganite with composition $Ni_{0.6}Cu_{0.4}Fe_yMn_{2-y}O_4$ where $0.1 \leq y \leq 0.5$ were synthesized by oxalate process. For this, the following reactants of analytical grade were used: nickel acetate, manganese acetate, cupric acetate and oxalic acid as starting materials and ferric chloride were used for the iron doping. The solution of nickel, manganese, copper acetates and ferric chloride was prepared in specific stoichiometry and added drop wise to hot (75 °C) oxalic acid solution with constant stirring. The prepared powder was dried at room temperature, pre-sintered at 350 °C for 3 h and mixed with PVA (polyvinyl alcohol) binder. The pellets were sintered at temperature 1000 °C in a muffle furnace for 8 h followed by cooling. The structure of $Ni_{0.6}Cu_{0.4}Fe_yMn_{2-y}O_4$ was confirmed by XRD Phillips PW 3710 diffractometer using Cr $K\alpha_1$ radiation. The crystal structure and the density related parameter of the samples were determined from the XRD data. The micro-structure was examined using scanning electron microscopy. The DC electrical resistivities for all the different compositions were measured by two-probe method. The commercially available Impedance Analyzer (solartron 1260A) in the frequency region 20 Hz to 1 MHz at room temperature was used for this measurement.

## 3. Results and discussion

### 3.1. TGA and DTA plots of oxalate precursor

Fig. 1 shows the TGA (thermo gravimetric analysis) and DTA (differential thermal analysis) plots of the oxalic co-precipitated for $Ni_{0.6}Cu_{0.4}Fe_{0.1}Mn_{1.9}O_4$ and $Ni_{0.6}Cu_{0.4}Fe_{0.5}Mn_{1.5}O_4$ ceramic oxalate precursor which thermally treated from room temperature to 1000 °C. From the TGA

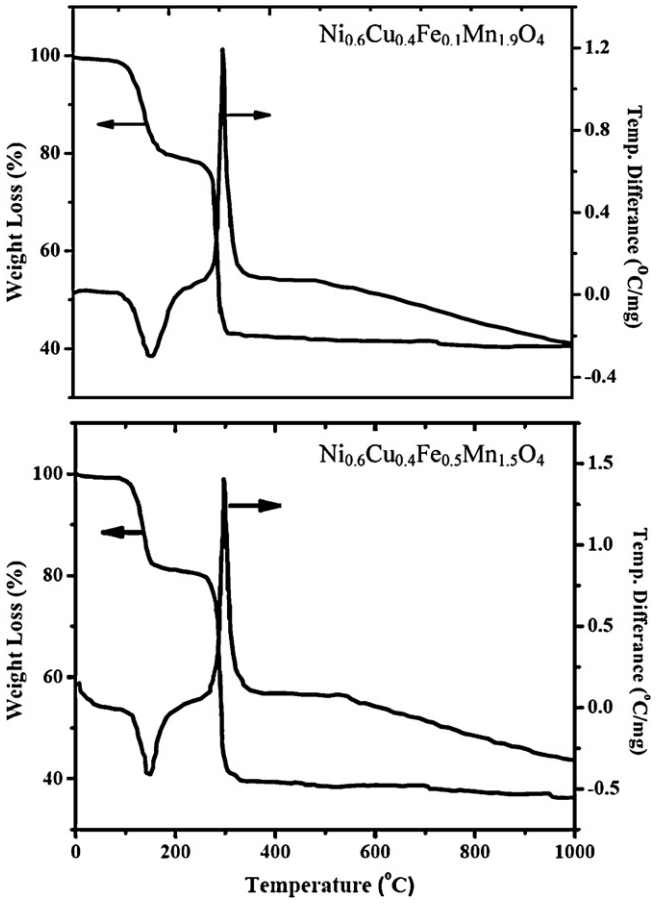


Fig. 1. TGA–DTA plots for the oxalic precipitate for expected NTC ceramic.

curve the initial weight loss of 20.19% up to temperature around 200 °C, accompanied with the exothermic reaction, is due to the removal of absorbed water molecule present in the precipitate. The major weight loss around 300 °C is due to the decomposition of the precipitate and formation of the ceramic. The exothermic peak in DTA at 318.37 °C supports the decomposition of precipitate around 350 °C. A slight weight gain from 350 °C to 750 °C (~3–4% which is not clearly observed in Fig. 1) is attributed to the oxidation of $Mn^{3+}$ cations on octahedral sites. When the temperature is further increased around 750 °C, the weight significantly decreased due to the reduction of $Mn^{4+}$ to $Mn^{3+}$ ions. Considering the TG/DTA analysis it can be inferred that the $Ni_{0.6}Cu_{0.4}Fe_yMn_{2-y}O_4$ ($0.1 \leq x \leq 0.5$) could be obtained by calcinations of oxalate precursors at temperatures higher than 750 °C.

### 3.2. Structural analysis

The X-ray diffraction (XRD) technique was used to confirm the presence of crystalline phases and to study the influence of atmosphere on the calcination process. The spinel structure of $Ni_{0.6}Cu_{0.4}Fe_yMn_{2-y}O_4$ ($0.1 \leq x \leq 0.5$) ceramic was confirmed by X-ray spectrum by predominant (3 1 1) plane which is shown in Fig. 2. These patterns confirm the formation of single cubic phase. The average crystallite size for the different compositions was calculated by Debye Sherrer's formula [19].

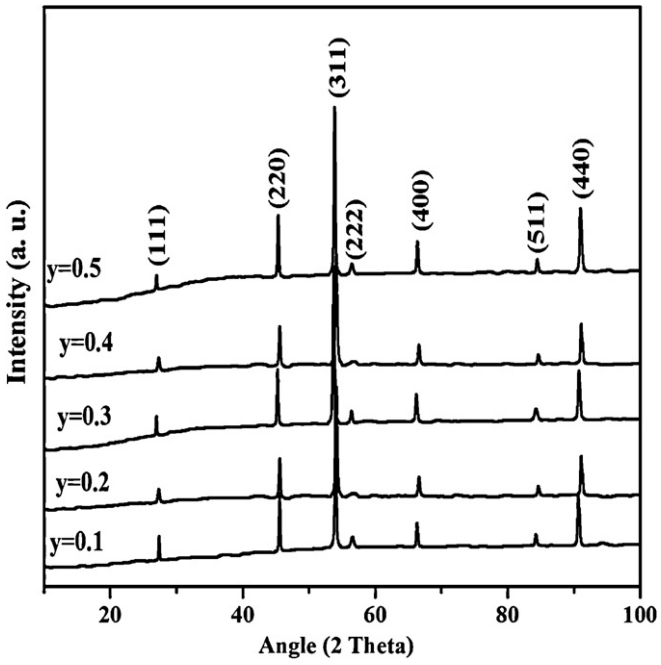


Fig. 2. X-ray diffraction pattern of $Ni_{0.6}Cu_{0.4}Fe_yMn_{2-y}O_4$ ($0.1 \leq y \leq 0.5$) NTC ceramic.

The variation in crystalline size depends upon the preparation condition which gives rise to different rates of nickel manganite formation for different concentration of iron. In $Ni_{0.6}Cu_{0.4}Fe_yMn_{2-y}O_4$ crystallite size shows irregular behavior with Fe doping. This may be attributed to the formation of $Fe^{2+}$ ions during the sintering process which has larger ionic radii than those $Fe^{3+}$ ions [20]. Due to this crystallite size increases in some samples.

The lattice parameters ($a$) of $Ni_{0.6}Cu_{0.4}Fe_yMn_{2-y}O_4$ for different iron concentration are tabulated in Table 1. It is seen that the lattice parameter decreases with increase in Fe concentration. This is due to the smaller radius of $Fe^{3+}$ (0.55 Å) as compared with $Mn^{3+}$ (0.58 Å) [21].

### 3.3. X-ray density

The X-ray density ($\rho_x$) was calculated by the formula [19],

$$\rho_x = \frac{8M}{Na^3}$$

where '$M$' is the molecular weight of composition, '$N$' is the Avogadro's number and '$a$' is the lattice parameter.

Table 1
Crystallite size, lattice parameter and X-ray density of $Ni_{0.6}Cu_{0.4}Fe_yMn_{2-y}O_4$ ($0.1 \leq y \leq 0.5$) NTC ceramic.

| NTC ceramic | Crystallite size (nm) | Lattice parameter (Å) | X-ray density (gm/cm$^3$) |
|---|---|---|---|
| $y = 0.1$ | 21.48 | 8.42 | 5.21 |
| $y = 0.2$ | 40.59 | 8.41 | 5.22 |
| $y = 0.3$ | 36.69 | 8.40 | 5.25 |
| $y = 0.4$ | 40.18 | 8.39 | 5.28 |
| $y = 0.5$ | 37.87 | 8.38 | 5.30 |

It was observed that the X-ray density increased with increase in iron concentration from 5.21 to 5.30 g/cm$^3$ in $Ni_{0.6}Cu_{0.4}Fe_yMn_{2-y}O_4$ ceramic which is tabulated in Table 1. It can be explained on the basis of Fe atom being heavier than the replaced Mn, leading to the increase in weight and also the X-ray density being inversely proportional to the lattice constant [22,23].

### 3.4. Sintered density

The sintered density ($\rho_s$) was calculated using the formula [19],

$$\rho_s = \frac{m}{\pi r^2 h}$$

where '$m$' is the mass of the pellet, '$r$' is the radius of the pellet and '$h$' is the thickness of the pellet.

The calculated sintered density ($\rho_s$) with iron concentration is shown in Fig. 3. The sintered density increased linearly with increase in Fe concentration from 5.21 to 5.30 g/cm$^3$ in $Ni_{0.6}Cu_{0.4}Fe_yMn_{2-y}O_4$ ceramic. This increase may be attributed to acceleration of cation inter diffusion due to Fe atom being heavier than the replaced Mn, leading to the increase in weight. It was also observed that X-ray density of each composition is larger than the corresponding sintered density. This is may be due to the existence of pores in the prepared samples.

### 3.5. Porosity

The porosity ($P$) for different compositions was calculated by the relation,

$$P = 1 - \frac{\rho_s}{\rho_x}$$

where $\rho_s$ and $\rho_x$ are defined above.

From X-ray density and sintered density the porosity of $Ni_{0.6}Cu_{0.4}Fe_yMn_{2-y}O_4$ NTC ceramic was calculated. The variation of sintered density and porosity related to iron

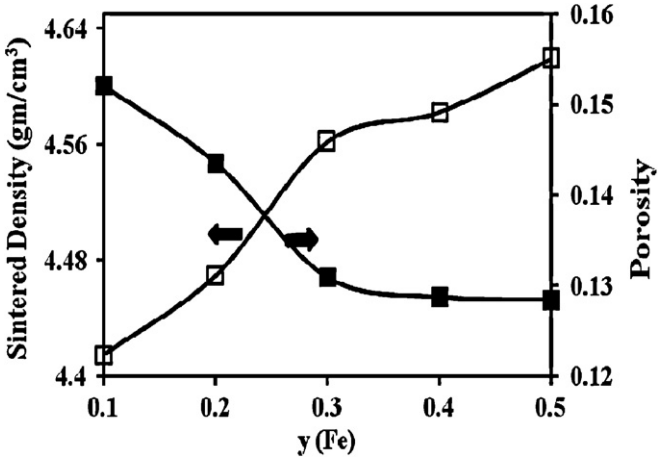


Fig. 3. Variation of sintered density (g/cm$^3$) and porosity with y (Fe) concentration in $Ni_{0.6}Cu_{0.4}Fe_yMn_{2-y}O_4$ NTC ceramic.

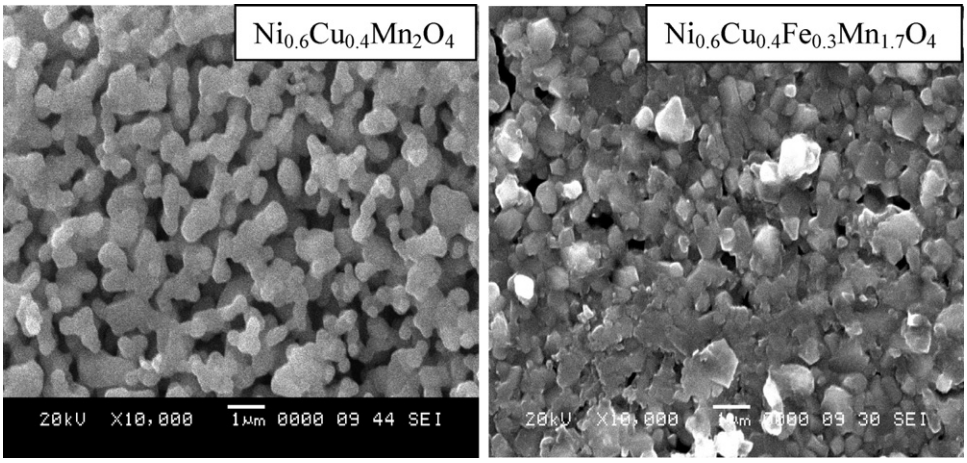


Fig. 4. SEM images of $Ni_{0.6}Cu_{0.4}Mn_2O_4$ and $Ni_{0.6}Cu_{0.4}Fe_{0.3}Mn_{1.7}O_4$ NTC ceramic.

concentration of NTC ceramic is shown in Fig. 3. It is observed that with the increase in iron content porosity decreased linearly from 0.15 to 0.12 for $Ni_{0.6}Cu_{0.4}Fe_yMn_{2-y}O_4$ respectively, which should be expected because of the reasons stated above.

As iron concentration increases the number of pores is reduced due to smaller grains the result of which the individual grains come closer to each other and the effective area of grain to grain contact increases. This in turn results in greater densification or lesser porosity which is observed from X-ray and sintered density and also in SEM images (SEM Fig. 4).

### 3.6. Surface morphology

The surface morphology of $Ni_{0.6}Cu_{0.4}Mn_2O_4$ and $Ni_{0.6}Cu_{0.4}Fe_{0.3}Mn_{1.7}O_4$ is shown in Fig. 4. The surface morphology of $Ni_{0.6}Cu_{0.4}Mn_2O_4$ [24] is also given here for comparison. From Fig. 4 it is observed that as Fe is doped in $Ni_{0.6}Cu_{0.4}Mn_2O_4$ it becomes denser. In case of $Ni_{0.6}Cu_{0.4}Fe_{0.3}Mn_{1.7}O_4$ the microstructure of the samples reveal well-grown grains with lower porosity. However, it is seen that the grain size of as-sintered ceramics decreases in the $Ni_{0.6}Cu_{0.4}Fe_{0.3}Mn_{1.7}O_4$ system, indicating that the doped Fe hindered the grain growth during sintering. This is caused by the dragging effect between the added $Fe^{3+}$ and the grain boundaries, which retards the grain growth [25]. Kingery et al. [26] have reported that when the effective concentration of dopants becomes greater than the solid solution limit, the energy for the movement of grain boundary increases and inhibits grain growth by a dragging effect.

### 3.7. DC electrical resistivity

Fig. 5 shows the relation between resistivity and absolute temperature of the $Ni_{0.6}Cu_{0.4}Fe_yMn_{2-y}O_4$ NTC ceramic. It is observed that in $Ni_{0.6}Cu_{0.4}Fe_yMn_{2-y}O_4$ NTC ceramic, the room temperature resistivity decreases with increase in temperature and Fe content. The room temperature resistivity of $Ni_{0.6}Cu_{0.4}Fe_yMn_{2-y}O_4$ NTC ceramic is 1 MΩ cm and 68 KΩ cm for $y = 0.1$ and $y = 0.5$ respectively. The relationship between $\log \rho$ and reciprocal of the absolute temperature $(1000/T)$ $K^{-1}$ for $Ni_{0.6}Cu_{0.4}Fe_yMn_{2-y}O_4$ NTC ceramic is shown in Fig. 6, which shows the linear relationship between these two parameters indicating the NTC behavior. The curve for $Ni_{0.6}Cu_{0.4}Mn_2O_4$ [24] is also given in the inset. The thermistor constant ($\beta_{30/90}$), activation energy, sensitivity index and stability factor are tabulated in Table 2.

The thermistor constant ($\beta_{30/90}$) was calculated by the equation [12],

$$\beta_{30/90} = \frac{\ln(R_{30}/R_{90})}{(1/T_{30}) - (1/T_{90})}$$

where $R_{30}$ and $R_{90}$ are resistivity measured at 30 °C and 90 °C respectively.

The activation energy was calculated using the equation $E = 2.303$ K slope of $\log \rho$ vs. $(1000/T)$ $K^{-1}$ curve. The

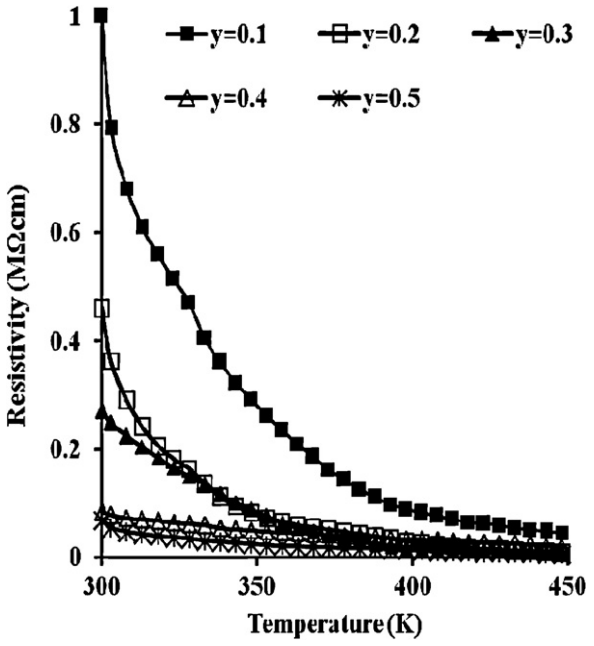


Fig. 5. Relationship between resistivity and absolute temperature of $Ni_{0.6}Cu_{0.4}Fe_yMn_{2-y}O_4$ $(0.1 \leq y \leq 0.5)$ NTC ceramic.

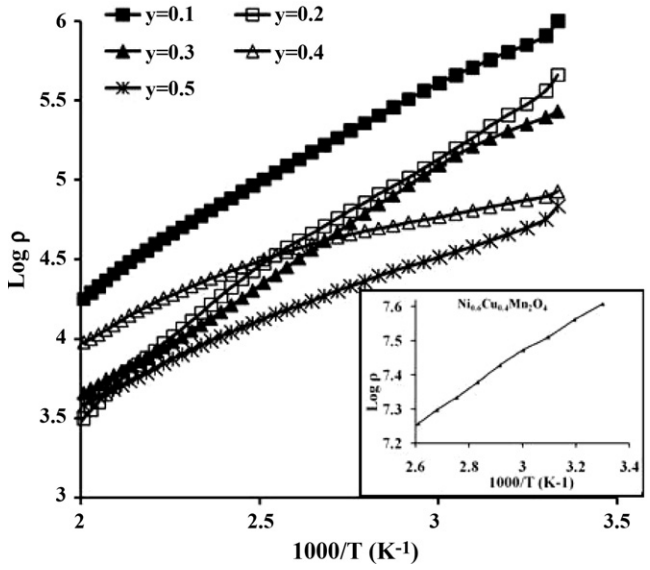


Fig. 6. Relationship between log $\rho$ and reciprocal of absolute temperature ($1000/T$) of $Ni_{0.6}Cu_{0.4}Fe_yMn_{2-y}O_4$ ($0.1 \leq y \leq 0.5$) with inset $Ni_{0.6}Cu_{0.4}Mn_2O_4$ [24] NTC ceramic.

sensitivity index ($\alpha$) and stability factor (SF) were calculated using the following formula [27],

$$\alpha = \frac{-\beta}{T^2}, \quad \mathrm{SF} = \log \frac{R_{\max}}{R_{\min}}$$

The $Ni_{0.6}Cu_{0.4}Fe_{0.1}Mn_{1.9}O_4$ NTC ceramics shows the coefficient of temperature sensitivity in the range ~3200 K which is in the industrial application range.

In nickel manganite the electrical conductivity does not depend only on the $Mn^{3+}$ and $Mn^{4+}$ concentration or hopping distance. For a given concentration of substituted transition metal ions, the configuration of ions in octahedral position also governs the conductivity. Indeed all the $Mn^{3+}$ ions do not participate in hopping process, to participate in hopping they need to have in their vicinity $Mn^{4+}$ ion. Therefore, the ordering between $Mn^{3+}$ and $Mn^{4+}$ and the presence of foreign ions on octahedral sites may disrupt the conduction [12]. Resistivity is actually the result of the combined factors such as grain size, crystal structure, imperfections and microstructure homogeneity. The high room temperature resistivity obtained in this work can be attributed to smaller grain size of the samples. Small grains imply larger number of insulating grain boundaries and hence greater energy barrier to electron conduction resulting thereby in higher resistivity.

The substitution of copper, nickel, cobalt for $Mn^{3+}$ ions leads to creation $Mn^{4+}$ ions in octahedral sites resulting in the change in ordering and increase in the conductivity. In case of $Ni_{0.6}Cu_{0.4}Fe_yMn_{2-y}O_4$ NTC ceramic the shape of the curves is modified with an increase in the iron content ($y$). For $y = 0.1$ a constant decrease of the resistivity can be noticed when the temperature increases until around 280 °C. Above this temperature and up to about 350 °C, the value of the resistivity becomes almost constant, as the conduction mechanisms, which are active below 280 °C achieve a kind of saturation. By the substitution of manganese by iron, the region of ''saturation'' seems to disappear and the curves are shifted toward lower resistivity's, making the material less resistive. However, the NTC-type behavior of NiCuFeMnO family is preserved. Similar kind of the results are reported by Veres et al. [28].

The activation energy is primarily the energy for hopping process from a cation $M^{n+}$ to $M^{(n+1)}$ on the octahedral sites and hence the mobility of the cations. It is well known that conduction is caused in nickel manganite by hopping of electron between $Mn^{3+}$ to $Mn^{4+}$ on octahedral sites. The activation energies calculated using the Arrhenius equation and from the specific resistivity values are tabulated in Table 2. The slope of the plot of the sample with $y = 0.4$ being so much different when compared with other plots might be due to a change in conduction mechanism. The conduction at low temperature is due to the hopping of electrons between $Fe^{2+}$ and $Fe^{3+}$ ions, whereas at high temperatures, it is due to polaron hopping. The activation energies show direct response to the changes in concentration of Fe substitution in nickel copper manganite because the substitution could change the energy band structure of the compound. The equation infers that the current carriers are generally electrons originated from $Fe^{2+}$ centers, which acts as electron donor. At higher temperatures the concentration of $Fe^{2+}$ ions increases along with increased hopping of holes generated from $Mn^{3+}$ and $Mn^{4+}$ ions transition. Similar results have been observed by Balaji et al. [29]. It is observed that as iron content increases ($y = 0.1$, 0.3, 0.5) in NiCu manganite activation energy decreases. In case of $y = 0.2$ and $y = 0.4$ the activation energy increases. The high activation energy is probably caused by the random distribution of the differently charged cations at octahedral sites [30]. It is clear that the concentration of $Fe^{2+}$-ions increases with decreasing Mn content which is in agreement with the fact that manganese does not suppress the ferrous ($Fe^{2+}$) ion formation. The increase of $Fe^{2+}$ ion concentration in manganite

Table 2
Composition dependent thermistor constant, activation energy, sensitivity index and stability factor of $Ni_{0.6}Cu_{0.4}Fe_yMn_{2-y}O_4$ NTC ceramic.

| NTC ceramic | Thermistor constant, $\beta$ (K) | Activation energy (eV) | Sensitivity index ($\alpha$) | Stability factor (SF) |
|---|---|---|---|---|
| $y = 0.1$ | 3208.74 | 0.3309 | 0.0357 | 0.8062 |
| $y = 0.2$ | 2521.21 | 0.3734 | 0.0283 | 0.4946 |
| $y = 0.3$ | 2473.77 | 0.2984 | 0.0275 | 0.6215 |
| $y = 0.4$ | 1937.48 | 0.3309 | 0.0215 | 0.4868 |
| $y = 0.5$ | 2081.15 | 0.2024 | 0.0231 | 0.5229 |

based on Ni and Cu leads to increase the conduction, due to electron hopping between $Fe^{2+}$ and $Fe^{3+}$ ions [20].

### 3.8. Dielectric constant

The dielectric constant of the bulk (pellet) samples was calculated from the capacitance (Cp) and loss factor (tan $\delta$) values measured in the frequency range 20 Hz to 1 MHz at room temperature. Silver paint (air dried) was coated on the flat surfaces to form electrodes for dielectric measurements. The dielectric constant of the samples was calculated from the capacitance (Cp) and loss factor (tan $\delta$) values measured Impedance Analyzer (solartron 1260A) in the frequency range 20 Hz to 1 MHz at room temperature. The compositional variation of dielectric constant ($\varepsilon'$) and loss factor (tan $\delta$) with frequency (20 Hz to 1 MHz) at room temperature is shown in Figs. 7 and 8 respectively. The curve for $Ni_{0.6}Cu_{0.4}Mn_2O_4$ [24] is also given in the inset (Fig. 7).

From Fig. 7 it is observed that the value of dielectric constant at lower frequency is much higher and increases with Fe concentration and decreases with frequency. It is observed that dielectric constant for $Ni_{0.6}Cu_{0.4}Fe_{0.1}Mn_{1.9}O_4$ at 20 Hz it is $\sim 9 \times 10^7$ and increases with Fe content up to $\sim 1.5 \times 10^9$ for $Ni_{0.6}Cu_{0.4}Fe_{0.5}Mn_{1.5}O_4$.

The mechanism of polarization in polycrystalline manganite is mainly reported due to the electron exchange interaction (hopping) between the $Mn^{3+}$ and $Mn^{4+}$ ions at the octahedral sites. This electron hopping appears to be favorable at lower applied ac electric field frequencies; the dielectric constant has therefore a maximum value at lower frequencies [31]. The variation of dielectric constant with frequency can be explained according to space charge polarization of Maxwell and Wagner

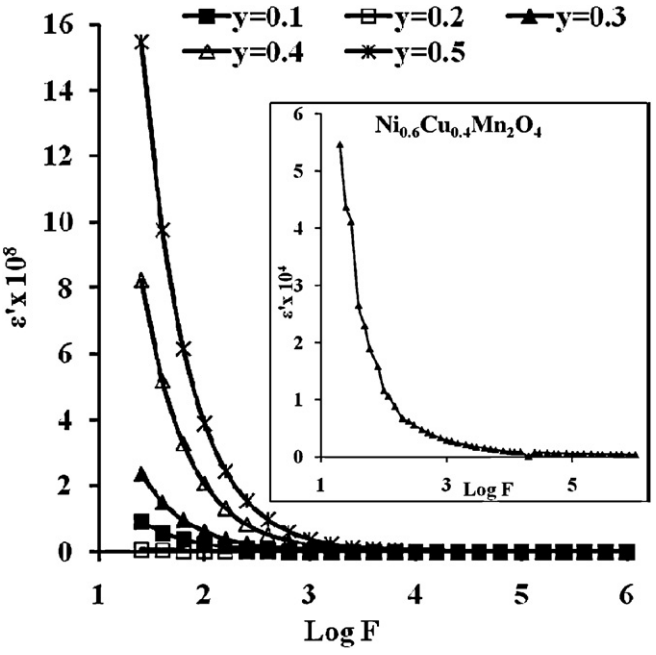


Fig. 7. Variation of dielectric constant ($\varepsilon'$) with frequency of $Ni_{0.6}Cu_{0.4}Fe_yMn_{2-y}O_4$ ($0.1 \leq x \leq 0.5$) with inset $Ni_{0.6}Cu_{0.4}Mn_2O_4$ [24] NTC ceramic.

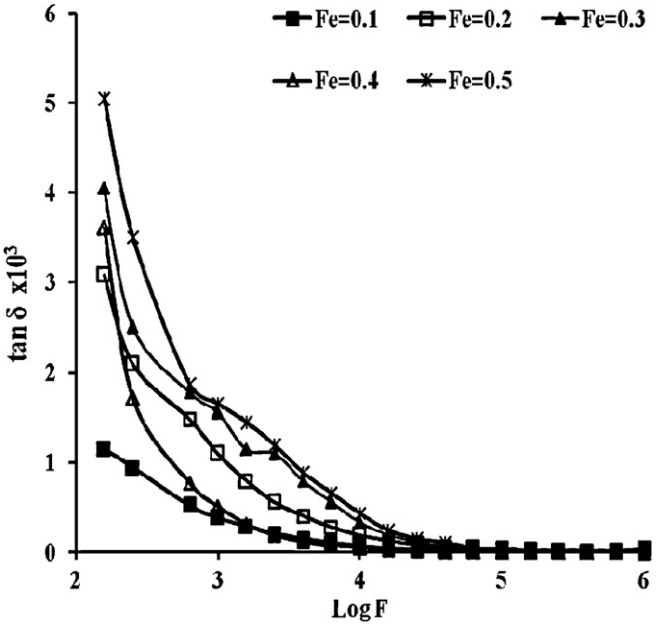


Fig. 8. Variation of loss factor (tan $\delta$) with frequency of $Ni_{0.6}Cu_{0.4}Fe_yMn_{2-y}O_4$ ($0.1 \leq x \leq 0.5$) NTC ceramic.

two layer model with Koop's phenomenological theory. According to this model the dielectric structure of the ceramic material is considered to be made up of two layers. The first layer consists of conducting grains and the second layer consists of poorly conducting grain boundaries. At lower frequencies the electrons at grain boundaries are more active than those in the grains, while at higher frequencies only the electrons in grains are active in electrical conduction. The electronic exchange between $Mn^{3+}$ and $Mn^{4+}$ is due to the local movement of electrons in the direction of electric field which determines the polarization in manganite. Polarization decreases with increase in frequency and then attains a constant value. It is because at higher frequencies the electrons exchange $Mn^{3+} \leftrightarrow Mn^{4+}$ cannot follow the alternation of the applied ac electric field hence $\varepsilon'$ and tan $\delta$ decreases [32].

For iron doped nickel copper manganite ceramic dielectric constant increases with increase in Fe content. According to Shitre et al. [33] the polarization in ferrites is through a mechanism similar to the conduction process. By the electro exchange between $Fe^{2+}$ and $Fe^{3+}$ ($Fe^{2+} \leftrightarrow Fe^{3+} + e^{-1}$), the local displacement of electrons in the direction of the applied electric field occurs and these electrons determine the polarization. The large value of dielectric constant at lower frequency is due to the predominance of species like $Fe^{2+}$ ions, interfacial dislocation pileups, oxygen vacancy, grain boundary defects, etc. The decrease in dielectric constant with increase in frequency is due to the fact that the polarization decreases with increasing frequency and then reaches a constant value. It was concluded that the electron exchange between $Fe^{2+}$ and $Fe^3$ ions results in the direction of an electric field, which might be responsible for electric polarization in Fe doped nickel copper manganite. The magnitude of exchange depends on the concentration of the $Fe^{3+}$–$Fe^{2+}$ ion pairs present at the B site.

Due to this as Fe concentration increases dielectric constant increases. The higher value of dielectric constant at lower frequency is due to voids, dislocations and other defects and due to dielectric loss increases.

The physical significance of tan δ is the energy dissipation in dielectric material that is proportional to imaginary part ($\varepsilon''$) of dielectric constant. The loss factor is considered to be caused by a domain wall resonance. When frequency increases, losses are found to be low if domain wall motion is inhibited and the magnetization is forced to change by rotation. It is observed that as copper and iron content increased dielectric constant also increased. The polarization is affected by some factors such as structural homogeneity, stoichiometry, density, grain size and porosity of the sample. The higher density of these compositions (when iron concentration increases) implies, decrease in the porosity and higher number of polarizing species per unit volume, both contributing to the observed increase in polarization [34]. When iron concentration increases in nickel manganite it results in a decrease in structural homogeneity of the manganite which may cause increase in polarization.

## 4. Conclusion

The doping of iron in $Ni_{0.6}Cu_{0.4}Fe_yMn_{2-y}O_4$ NTC ceramic produces appreciable changes in the structural, electrical and dielectric properties. The grain size and porosity decreases systematically with iron content. The room temperature resistivity decreases with increase in iron content and thermistor constant are in industrial application level make these compounds promising for high temperature NTC type thermistor applications, with tunable range of sensitivity. The dielectric constant of low frequency at room temperature increases with iron content in nickel copper manganite and decreases with frequency from $\sim 9 \times 10^7$ to $1.5 \times 10^9$ at 20 Hz. The value of dielectric constant at 1 KHz was $\sim 1.2 \times 10^6$ increases up to $3.8 \times 10^7$ and $3 \times 10^3$ to $9 \times 10^3$ at 1 MHz respectively with increase in iron concentration. The high dielectric constant might be used in capacitors of dynamic random access memories (DRAM) for personal computers and workstations which strongly suggests that $Ni_{0.6}Cu_{0.4}Fe_yMn_{2-y}O_4$ NTC ceramics can be a good candidate for applications where high dielectric constant with low loss in radio-frequency range are required.

## Acknowledgments

Author R.N. Jadhav would like to express thanks to DST for the Award of Women Scientist-A (WOS-A). One of the authors Vijaya Puri gratefully acknowledges the UGC India for Award of Research Scientist 'C'.

## References

[1] J.G. Fagan, V.R.W. Amarakoon, Reliability and reproducibility of ceramic sensors. 1. NTC thermistors, Am. Ceram. Soc. Bull. 72 (1993) 70–79.

[2] G. Lavenuta, Negative temperature coefficient thermistors, Sensors 14 (1997) 46–55.

[3] C.H. Zhao, B.Y. Wang, P.H. Yang, L. Winnubst, C.S. Chen, Effects of Cu and Zn co-doping on the electrical properties of $Ni_{0.5}Mn_{2.5}O_4$ NTC ceramics, J. Eur. Ceram. Soc. 28 (2008) 35–40.

[4] A. Veres, J.G. Noudema, O. Perez, S. Fourrez, G. Bailleul, The effect of manganese substitution to gallium on the physical properties of $MgGa_{2-x}Mn_xO_4$ spinel type ceramic thermistors, J. Eur. Ceram. Soc. 27 (2007) 3873–3876.

[5] K. Park, J. Lee, S. Kim, W. Seo, W. Cho, C. Lee, S. Nahm, The effect of Zn on the microstructure and electrical properties of $Mn_{1.17-x}Ni_{0.93-}Ni_{0.93}Co_{0.9}Zn_xO_4$ ($0 \le x \le 0.075$) NTC thermistors, J. Alloys Compd. 467 (2009) 310–316.

[6] K. Park, Fabrication and electrical properties of Mn–Ni–Co–Cu–Si oxides negative temperature coefficient thermistors, J. Am. Ceram. Soc. 88 (2005) 862–866.

[7] C. Zhao, B. Wang, P. Yang, L. Winnubst, C. Chen, Effects of Cu and Zn co-doping on the electrical properties of $Ni_{0.5}Mn_{2.5}O_4$ NTC ceramics, J. Eur. Ceram. Soc. 28 (2008) 35–40.

[8] S.A. Kanade, V. Puri, Electrical properties of thick-film NTC thermistor composed of $Ni_{0.8}Co_{0.2}Mn_2O_4$ ceramic: effect of inorganic oxide binder, Mater. Res. Bull. 43 (2008) 819–824.

[9] S.M. Savic, M.V. Nikolic, O.S. Aleksic, M. Slankamenac, M. Zivanov, P.M. Nikolic, Intrinsic resistivity of sintered nickel manganite vs. powder activation time and density, Sci. Sin. 40 (2008) 27–32.

[10] W. Wang, X. Liu, F. Gao, C. Tian, Synthesis of nanocrystalline $Ni_1Co_{0.2}Mn_{1.8}O_4$ powders for NTC thermistor by a gel auto-combustion process, Ceram. Int. 33 (2007) 459–462.

[11] M. Hosseini, The effect of cation composition on the electrical properties and aging of Mn–Co–Ni thermistors, Ceram. Int. 26 (2000) 245–249.

[12] K. Park, I.H. Han, Effect of $Cr_2O_3$ addition on the microstructure and electrical properties of Mn–Ni–Co oxides NTC thermistors, J. Electroceram. 17 (2006) 1069–1073.

[13] J.M. Varghese, A. Seema, K.R. Dayas, Microstructural electrical and reliability aspects of chromium doped Ni–Mn–Fe–O NTC thermistor materials, Mater. Sci. Eng. B 149 (2008) 47–52.

[14] S.A. Kanade, V. Puri, Properties of thick film $Ni_{0.6}Co_{0.4}Fe_yMn_{2-y}O_4$: ($0 \le y \le 0.5$) NTC ceramic, J. Alloys Compd. 475 (2009) 352–355.

[15] W.A. Groen, C. Metzmacher, P. Huppertz, S. Schuurman, J. Electroceram. 7 (2001) 77.

[16] D.L. Fang, C.S. Chen, A.J.A. Winnubst, J. Alloys Compd. 454 (2008) 286.

[17] Srrias, S. Bayonne, A. Rousset, X. Alcobe, M.L.M. Sarrion, Solid State Ionics 128 (2000) 233.

[18] K. Park, D.Y. Bang, J.G. Kim, J.Y. Kim, C.H. Lee, B.H. Choi, J. Korean Phys. Soc. 41 (2002) 251.

[19] M. Ajmal, A. Maqsood, Influence of zinc substitution on structural and electrical properties of $Ni_{1-x}Zn_xFe_2O_4$ ferrites, Mater. Sci. Eng. B 139 (2007) 164–170.

[20] A.A. Sattar, H.M. El-Sayed, K.M. El-Shokrofy, M.M. El-Tabey, Study of the dc resistivity and thermoelectric power in Mn-substituted Ni–Zn ferrites, J. Mater. Sci. 42 (2007) 149–155.

[21] Z. Wang, C. Zhao, P. Yang, A.J.A. Winnubst, C. Chena, X-ray diffraction and infrared spectra studies of $Fe_xMn_{2.34-x}Ni_{0.66}O_4$ ($0 < x < 1$) NTC ceramics, J. Eur. Ceram. Soc. 26 (2006) 2833–2837.

[22] Q. Wei, J. Lie, Y. Chen, Cation distribution and infrared properties of $Ni_xMn_{1-x}Fe_2O_4$ ferrites, J. Mater. Sci. 36 (2001) 5115–5118.

[23] U. Ghazanfara, S.A. Siddiqia, G. Abbas, Structural analysis of the Mn–Zn ferrites using XRD technique, Mater. Sci. Eng. B 118 (2005) 84–86.

[24] R.N. Jadhav, V. Puri, Influence of copper substitution on structural, electrical and dielectric properties of $Ni_{(1-x)}Cu_xMn_2O_4$ ($0 \le x \le 1$) ceramics, J. Alloys Compd. 507 (2010) 151–156.

[25] H. Zhang, A. Chang, C. Peng, Preparation and characterization of $Fe^{3+}$-doped $Ni_{0.9}Co_{0.8}Mn_{1.3-x}Fe_xO_4$ ($0 \le x \le 0.7$) negative temperature coefficient ceramic materials, Microelectron. Eng. 88 (2011) 2934–2940.

[26] W.D. Kingery, H.K. Bowen, D.R. Uhlmann, Introduction to Ceramics, 2nd ed., John Wiley & Sons, Singapore, 2004.

[27] S. Jagtap, S. Rana, U. Mulik, D. Amalanekar, Thick film NTC thermistor for wide range of temperature sensing, Microelectron. Int. 24 (2007) 7–13.
[28] A. Veres, J.G. Noudem, S. Fourrez, G. Bailleul, The influence of iron substitution to manganese on the physical properties of $YMnO_3$, Solid State Sci. 8 (2006) 137–141.
[29] S. Balaji, R. Kalai Selvan, L.J. Berchmans, S. Angappan, K. Subramanian, C.O. Augustin, Combustion synthesis and characherrization of $Sn^{4+}$ substituted nanocrystalline $NiFe_2O_4$, Mater. Sci. Eng. B 119 (2005) 119–124.
[30] K. Park, Structural and electrical properties of $FeMg_{0.7}Cr_{0.6}Co_{0.7-x}Al_xO_4$ ($0 \leq x \leq 0.3$) thick film NTC thermistors, J. Eur. Ceram. Soc. 26 (2006) 909–914.
[31] M. Iqbal, Z. Ahmed, Electrical and dielectric properties of lithium manganate nanomaterials doped with rare-earth elements, J. Power Sources 179 (2008) 763–769.
[32] S. Angappan, L.J. Berchmans, C.O Augustin, Sintering behaviour of $MgAl_2O_4$ a prospective anode material, Mater. Lett. 58 (2004) 2283–2289.
[33] A.R. Shitre, V.B. Kawade, G.K. Bichile, K.M. Jadhav, X-ray diffraction and dielectric study of $Co_{1-x}Cd_xFe_{2-x}Cr_xO_4$ ferrite system, Mater. Lett. 56 (2002) 188–193.
[34] M. Dimri, A. Verma, S. Kashyap, D. Dube, O. Thakur, C. Prakash, Structural, dielectric and magnetic properties of NiCuZn ferrite grown by citrate precursor method, Mater. Sci. Eng. B 133 (2006) 42–48.